Dr. Uğur Akman, Assoc. Prof.
Department of Chemical Engineering
Boğaziçi University, Bebek 80815, İstanbul - Turkey
Tel: +90 (212) 2631540 - 1867, Fax: +90 (212) 2872460
E-Mail: akman@boun.edu.tr

Nonlinear Model Predictive Control of Retrofit Heat-Exchanger Networks

Uğur Akman
Department of Chemical Engineering, Boğaziçi University, Bebek 80815, İstanbul - Turkey

Abstract – Control of a retrofit Heat-Exchanger Network (HEN) was studied within the framework of Nonlinear Model Predictive Control (NMPC). For this purpose, an optimal retrofit design of the HEN was performed, and thus, bypasses as control variables were placed in order to satisfy steady-state hard/soft target-temperature constraints. Control configuration was determined and tested under decentralized feedback-control scheme which did not satisfy the constraints. The NMPC scheme, in which the nonlinear distributed-parameter HEN model was solved sequentially, satisfied all the temporal and steady-state hard/soft target-temperature constraints. A version of the classical NMPC scheme, in-lined with piecewise-continuous control-vector parameterization, showed a superior performance with regard to smoothness of the response and significant reduction in computation time.

Keywords: *retrofit HEN, NMPC, NMPC with piecewise-continuous control-vector parameterization*

Introduction

A HEN, synthesized for nominal conditions, must also be flexible and resilient to disturbances in its source streams to be able to control the network`s target-stream temperatures at desired values or within a permissible range. The degrees of freedom required to achieve control objectives can only be introduced by bypass and/or split streams [1,2]. A method for optimal retrofit design (ORD) of HENs that do not posses control variables in their original structures has already been presented [1,2,3,4]. In the ORD method, bypasses, as control variables, are placed in order to satisfy hard/soft target-temperature constraint specifications at the steady-state operating conditions, with minimum increase in exchanger areas (minimum retrofit-design cost). In ORD, alternative bypass-placement configurations are to be compared in terms of static flexibility, cost of retrofit design, and resiliency, e.g., the Morari Resiliency Index (MRI) [4], and pairings among the bypasses and controlled target temperatures are to be selected for the most favorable configuration according to the Relative Gain Array (RGA) criterion [4]. With the ORD formulation [1,2,4], when the set of external disturbances entering the HEN are measured, optimal values of the target temperatures and bypass openings that guarantee steady-state feasibility of the new operating point can be calculated. This optimal solution also guarantees that the constraints on target-stream temperatures are satisfied as much as the network structure allows (more likely for soft, but less likely for hard constraints) [1,4]. The remaining task is to determine how to apply, in time, the set of optimal bypass openings (controls) so that the HEN's dynamic response in reaching the final steady-state feasible operating point is acceptable. A control scheme to be applied to a retrofit HEN should therefore be able to: • *accommodate requirements of the optimal retrofit design,* • *match the optimal nominal operating conditions of the HEN exactly under zero-disturbance,* • *satisfy all hard/soft target-temperature constraints for all possible disturbance directions at any post-disturbance steady-state feasible operating point,* • *satisfy all temporal hard/soft target-temperature constraints for all possible disturbance directions in transition from pre- to post-disturbance steady-state feasible operating points.* For the control of retrofit HENs, the nonlinear-model-based predictive-control (NMPC) scheme should offer great flexibilities in satisfying the above-mentioned requirements. Therefore, in this work, control of a retrofit HEN has been studied within the framework of NMPC.

Optimal Retrofit Design (ORD) of HENs

The major problem in control of HENs is the lack of sufficient number of variables to manipulate in order to achieve control objectives. All necessary control actions in order to satisfy target-temperature constraints should be taken using stream splits and/or bypasses that may/should be present in a HEN. Unfortunately, static HEN synthesis methods do not allocate bypass streams and generally yield structures which do not contain any or enough number of stream splits. Placement of bypass streams to a pre-designed HEN in favor of its control creates a cost/controllability trade-off problem (addition of bypasses on exchangers requires area increases) the solution of which requires an optimal retrofit design. Once the number and location of the bypass streams are decided on, a HEN can be redesigned without changing its original structure in order to increase its static and dynamic flexibility against external disturbances. The objectives of the retrofit design can be set as follows [4]: • *it should be a minimum cost (total network area) design,* • *it should yield the nominal operating conditions of the HEN exactly under zero-disturbance case (e.g., be a maximum-energy-recovery network),* • *it should posses maximum flexibility in each disturbance direction,* • *it should satisfy target-temperature constraints for all disturbance directions.*

Formulation of the ORD problem is summarized by Eqs.(1-5) [4]. The decision variables to achieve these objectives are the bypass fractions (a different set for each disturbance direction) and the increments in heat-exchanger areas (common for each disturbance direction). Disturbance directions are identified by index *k*. The zero-disturbance direction (nominal operating condition of the retrofit design) is identified by *k=0*. Equality constraints, Eq.2, guarantee that the target temperatures of the HEN under zero disturbance will exactly be those at the nominal operating condition. Inequality constraints, Eq.3, guarantee that the target-temperature range constraints are satisfied for all disturbance directions. Side constraints, Eq.5, put lower and upper limits on bypass openings only at zero-disturbance direction. Inequality constraints, Eq.4, limit the bypass openings, for each non-zero disturbance direction, between a certain fraction of openings of the corresponding bypasses at the nominal operating condition of the retrofit design (*k=0*).

objective function:	$\underset{S^k,\,\mathbf{u}^j,\,\mathbf{A}}{\textit{maximize}} \left\{ \sum_k S^k \Big/ \sum_n A_n \right\}$	k=1,...,N_d	j=0,...,N_d	(1)
equality constraints:	$\mathbf{T}^{t,k} - \overline{\mathbf{T}}^t = 0$	k=0		(2)
inequality constraints:	$\overline{\mathbf{T}}^t - \Delta\mathbf{T}^t \le \mathbf{T}^{t,k} \le \overline{\mathbf{T}}^t + \Delta\mathbf{T}^t$	k=1,...,N_d		(3)
	$(1-r)\mathbf{u}^0 \le \mathbf{u}^j \le (1+r)\mathbf{u}^0$	j≠0	k=1,...,N_d	(4)
side constraints:	$u^{min} \le \mathbf{u}^j \le u^{max}$	j=0		(5)

$\mathbf{u}^{min}$ and $\mathbf{u}^{max}$ for the nominal operating conditions (under zero disturbance) of the retrofit design should be set by considering the realizability of the retrofit design. The upper limit should not be very high considering the bypass-line and valve sizing, yet it should not be very low considering the flexibility and resiliency of the retrofit design. Similarly, the lower limit should not differ very much from the upper limit considering the bypass-line and valve sizing. When only the cost of retrofit design (incremental exchanger areas) is considered, it may be thought

to set the lower limits of the nominal bypass openings of the retrofit design to zero. However, there are trade-offs between the design cost, flexibility, and resiliency of HENs. Depending on the direction of a particular disturbance, some disturbances can be rejected or re-directed favorably only by decreasing bypass openings, and if some or all bypass openings at the nominal operating conditions of the retrofit design are zero, the retrofit HEN may not reject, or tolerate disturbances as much as desired.

Static flexibility, S^k, can be defined as the magnitude of the maximum disturbance (e.g., ± directed changes in source temperatures) that a structure can tolerate at steady state within prescribed operational limits (hard/soft target-temperature constraints). Determination of the flexibility of a structure is a static constrained nonlinear optimization problem, and for all disturbance directions, is directly obtained as the solution to the optimal retrofit design problem (Eqs.1-5).

Selection and Pairing of Manipulated and Controlled Variables

The success of the retrofit design summarized above depends upon the decisions made on the number and location of bypass streams. If a feedback-control scheme is thought, then the number of bypass streams (manipulated variables) are selected equal to the number of target streams, N_t, (controlled variables), the temperatures of which have to be controlled. Since a bypass can be placed on either the hot and/or cold side of an exchanger, and if there are N_{HEX} exchangers in the HEN, there exist $C\{2\times N_{HEX}\ ,\ N_t\}$ (combination of $2\times N_{HEX}$ locations taken N_t at a time) alternative bypass-placement configurations [5]. Each of these configurations results in alternative retrofit designs with different flexibilities and different controllability and resiliency characteristics.

The static flexibility measure, S^k, for each alternative, and for all disturbance directions, is directly obtained as the solution to the optimal retrofit-design problem (Eqs.1-5). Dynamic flexibility of each alternative may be assessed, for example, by evaluating their MRI values. Final decision on selection of manipulated variables can than be made on the basis of comparative analysis of these flexibility and resiliency indices. After selecting the bypass locations on the basis of MRI, the remaining task is to decide on the pairings of these bypasses with the controlled target temperatures. With N_t bypasses and N_t target temperatures there are $N_t!$ (factorial) pairing possibilities most of which can be eliminated just by inspection [5]. The remaining possibilities may be analyzed using the RGA technique, to select the pairings that minimize closed-loop interactions, based on steady-state gain matrix of the HENs. For HENs, RGA favors direct pairings among bypasses and target temperatures [4].

Steady-State Optimal Control (SSOC) of Retrofit HENs

With regard to a HEN, the control objective is to keep target-stream temperatures either exactly at the nominal conditions for which the HEN has been designed (hard targets) or as close as possible to the nominal conditions (soft targets). Generally, without a retrofit design, all of the hard targets may not be satisfied for an arbitrary disturbance, since flexibility (disturbance-rejection ability) at/around this nominal design point is not considered during traditional static design. Instead, an alternative operating point around the nominal operating conditions may be targeted. However, not all operating points around the nominal conditions are feasible. The ORD formulation described above increases the region of feasible operation (owing to addition of bypasses and area increases with an aim to maximize static flexibility). Therefore, after ORD, for a measured disturbance, feasible targets must be selected based on the retrofit design. Once this feasible operating point is identified, the remaining control task is to drive the system from its nominal operating conditions to the new feasible operating point (post-disturbance target) after a disturbance.

The static optimization (steady-state optimal control, SSOC) problem can be defined as follows. When the HEN experiences disturbances in source-stream temperatures (or flowrates), find a set of bypass fractions that will minimize the total deviations in the target temperatures, subject to steady-state target-temperature constraints (soft/hard) and manipulated-variable bounds, such that the HEN remains feasible. If the magnitude of the disturbance is less than or equal to the flexibility index, S^k, obtained from the solution of the ORD problem (Eqs.1-5) corresponding to this particular disturbance direction, then it is guaranteed that the SSOC problem will have a feasible solution. Formulation of the steady-state optimal control problem is summarized by Eqs.(6-8) [1].

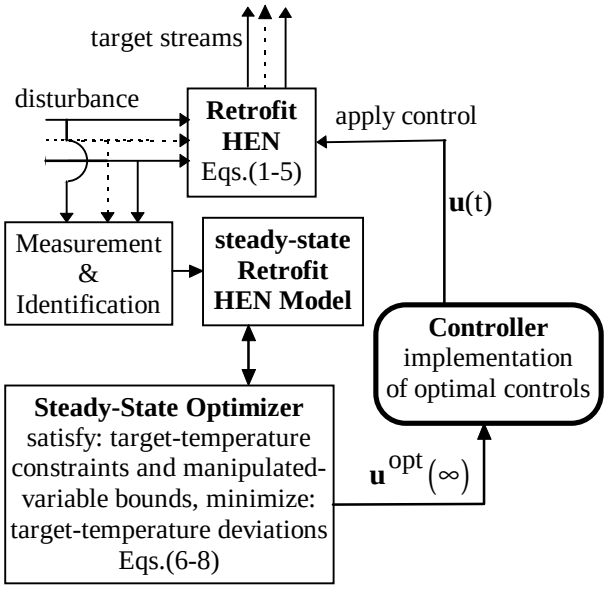


Figure 1. Open-loop steady-state optimal control scheme (SSOC) for retrofit HENs.

$$\text{objective function:} \quad \underset{\mathbf{u}}{minimize} \ \left\| \Delta \mathbf{T}^t \right\| \tag{6}$$

$$\text{soft/hard target constraints:} \quad \Delta \mathbf{T}^t_{min} \le \Delta \mathbf{T}^t \le \Delta \mathbf{T}^t_{max} \tag{7}$$

$$\text{manipulated-variable bounds:} \quad (1-r)\mathbf{u}^0 \le \mathbf{u} \le (1+r)\mathbf{u}^0 \tag{8}$$

This centralized steady-state-model-based optimal open-loop control scheme is depicted in Fig.1. In this scheme, temperatures (disturbances) of the source streams entering the HEN are measured/identified. These measurements are fed to the optimizer that performs a static optimization by referring to the steady-state algebraic model of the HEN. The optimizer finds the optimal values of the bypass fractions such that the target-temperature constraints and manipulated-variable bounds are satisfied, and deviations in target-temperatures from their nominal values are minimized. Assuming that there is no mismatch between the static model of the optimizer and the process at the steady state, the remaining task is to select how to implement the optimal controls in time (how to reach $\mathbf{u}^{opt}(\infty)$).

A Sample HEN

The specific HEN problem used in this work is defined in Table 1. There exist alternative solutions to this problem in the literature. The structure shown in Fig.2 (the cooler that is present in the original structure has not been included) has been obtained from an MINLP algorithm [6].

Table 1. Definition of the HEN problem.

Stream	W (kW/K)	T^s(K)	T^t(K)
Hot-1	10	620	385
Hot-2	15	720	400
Cold-1	20	300	560
Cold-2	30	280	340

ΔT^a = 10 K, U_n = 0.5 kW/m^2-K

The structure shown in Fig.2 can tolerate ± directed source-temperature disturbances with a magnitude of at most 5K (the minimum of the maximum flexibilities in each disturbance direction) when all the target temperatures are constrained within ±5K [5]. This static flexibility of 5K indicates that, the structure guarantees not to require any control if the control objective is to keep the target temperatures within ±5K, as long as the disturbance entering the network from the "worst" disturbance direction is at most 5K in magnitude. However, among the 16 possible disturbance directions which do not include zero disturbance in any of the source streams (four disturbance sources and two, + and –, directions), the structure, in its particular "best" disturbance direction, can tolerate source-temperature disturbances with magnitudes at most ±7.9K, respectively.

The control, and hence, the resiliency (dynamic flexibility) problems arise when the operational limits are tightened (e.g., ±0K deviation in target temperatures) and/or when disturbances are expected in larger magnitudes. Once the number and location of the bypass streams are decided on, a HEN can be redesigned without changing its original structure in order to increase its static and dynamic flexibility against external disturbances. The optimal retrofit design (ORD) formulation, Eqs.(1-5), described previously can be applied for each one of the bypass-location alternatives individually to obtain alternative retrofit HENs (having identical structures but different exchanger areas and different nominal bypass openings) with greater steady-state flexibility. Then, to select the best bypass-location set which should also increase the dynamic flexibility, MRI of these alternative retrofit designs can be calculated based on steady-state model of the HEN. After such selection of bypass locations, the pairings among the controlled target temperatures and the bypasses can be decided on using the RGA criterion based on the steady-state model of the HEN.

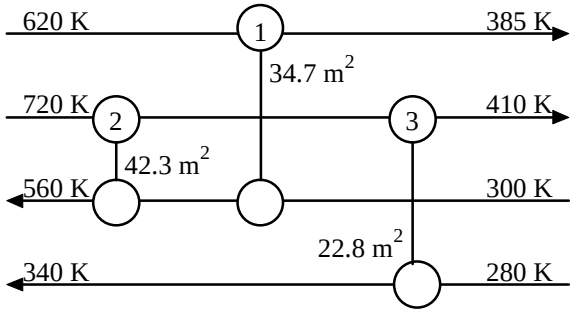


Figure 2. Original HEN structure and design [4].

Fig.3 shows the final retrofit design of the HEN, location of bypasses, optimal nominal (under zero disturbance) bypass openings, and pairings among controlled temperatures and manipulated bypasses. The locations of the bypasses are those that give the maximum MRI value and, at the same time, relatively low retrofit cost (total area increase) [4]. The static flexibility of the retrofit HEN is again 5K for the "worst" disturbance direction, however, in its "best" disturbance direction, the retrofit HEN can now tolerate disturbances with magnitudes at most ±12.4K [4].

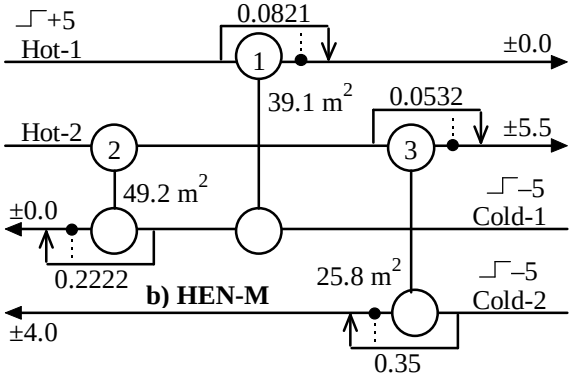


Figure 3. Retrofit HEN [4].

Dynamic Model of Heat Exchangers

For the dynamic modeling, single-tube-pass, shell-and-tube exchangers were chosen. The design parameters were evaluated using a detailed design algorithm [7,8]. The distributed-parameter model of the heat exchangers, given by Eqs.(9-10), were used to construct the dynamic model of the HEN by connecting the PDEs of the individual exchangers through boundary conditions. Eqs.(11-12) describe the energy balances at the bypass-mixing points that are assumed algebraic (instantaneous mixing). Utilizing the "method of lines" numerical technique, the PDEs were discretized in z-direction using "five-point biased-upwind" finite-difference formulas, which eliminated steady-state offset problem, and thus, converted into ODEs.

$$\frac{\partial T_H}{\partial t} = -v_H \frac{\partial T_H}{\partial z} + \frac{h_H a_H h_C a_C}{h_C a_C + h_H a_H} \frac{(T_C - T_H)}{A_H \rho_H C_{p_H}} \tag{9}$$

$$\frac{\partial T_C}{\partial t} = +v_C \frac{\partial T_C}{\partial z} + \frac{N_T h_C a_C h_H a_H}{h_C a_C + h_H a_H} \frac{(T_H - T_C)}{A_C \rho_C C_{p_C}} \tag{10}$$

bypass mixing cold side: $$T_C^t = T_C^o u_C + T_C(1-u_C) \tag{11}$$

bypass mixing hot side: $$T_H^t = T_H^o u_H + T_H(1-u_H) \tag{12}$$

Nonlinear Model Predictive Control (NMPC) of Retrofit Heat-Exchanger Networks

The objective in this section is to apply the Nonlinear Model Predictive Control (NMPC) technique [9,10,11] to control of HENs by selecting a set of future control moves (bypass openings) in the control horizon to minimize a function (norm of the target-temperature deviations from predicted optimal/feasible post-disturbance steady-state values) over a prediction horizon in which both the dynamic and steady-state model of the HEN are utilized subject to temporal and steady-state target constraints and manipulated-variable bounds. The general NMPC approach that is applicable to control of retrofit HENs is depicted in Fig.4.

The NMPC scheme for control of retrofit HENs is depicted in Fig.5. The mathematical formulation of the general NMPC approach for control of HENs can be described by Eqs.(13-24).

The objective function (Eq.13) is the norm of the residuals between the outputs (target temperatures) predicted by the HEN model and the set points (optimal/feasible post-disturbance steady-state target temperatures) over the prediction horizon of R time steps. The decision variables are the control actions considered only m time steps into the future ($m < R$). After the m^{th} time step control action is constant (Eq.22). The absolute bounds on the manipulated variables (Eq.19) are in accordance with those used in the formulation of the optimal steady-state control problem (Eq.8). The velocity constraints on the manipulated variables are defined by Eqs.(20-21) where changes in the bypass openings are bounded within $\pm r^*$ fraction of the nominal bypass openings of the retrofit design. Eq.18 defines the temporal target-temperature constraints that should be in agreement with the target constraints used in the formulation of the optimal steady-state control problem (Eq.7). In the algorithm, only the first of the control actions, optimized over the prediction horizon, is implemented and the outputs (target temperatures) of the plant (actual HEN) are measured. Compensation of the plant/model mismatch is considered in Eqs.(14-15) where the difference between the model output and the plant output at the current time step k is used to predict the output over the prediction horizon R. Eq.16 specifies the set of ODEs obtained after discretization of the PDEs (Eqs.9-10) describing the HEN dynamics. Eq.17 indicates the temperature profiles in the exchangers at the beginning of the k^{th} time step which are obtained

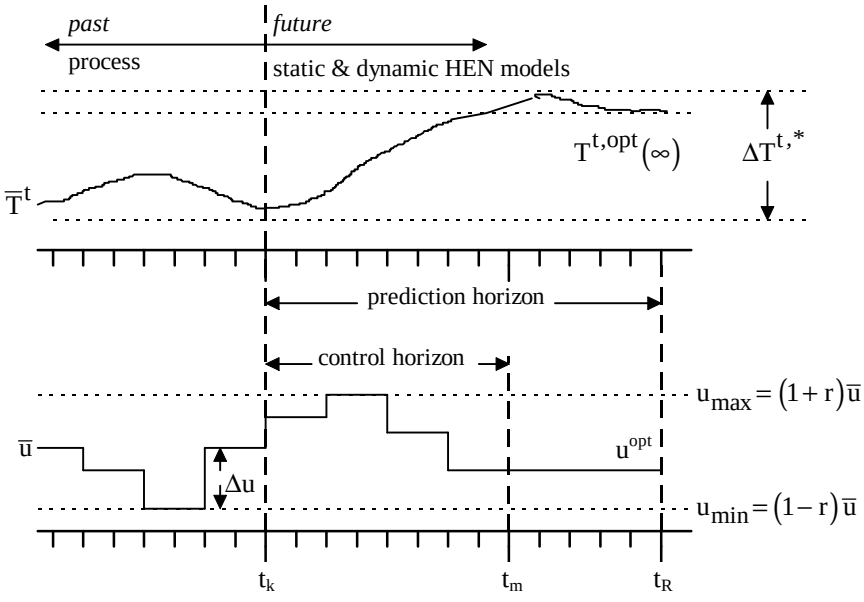


Figure 4. General NMPC approach in control of retrofit HENs.

from the solution of the model over the previous time step, based on the bypass openings actually implemented on the plant. The path constraints (Eq.18) are converted into a terminal equality constraint (Eq.24) by augmenting the set of ODEs with the single ODE given by Eq.23 [12].

NMPC with Sliding Piecewise-Continuous Control-Vector Parameterization (NMPC/SPCCVP)

A — Local Parameterization (SPCCVLP):

For systems, like HENs, where a manipulated variable (bypass) is directly linked to a controlled (target) stream, the stepwise movements of manipulated variables in NMPC may result in a kinky response in controlled variables. The response can be made smoother if the manipulated variables are parameterized as piecewise-continuous time-dependent functions in the prediction horizon (spline points $t_i,...,t_{i+m-1}$) and the first spline of each of the manipulated variables is applied in a sliding mode to the plant at t_k. In general, the success depends on the functional form of the parameterization. Higher order parameterizations may perform better, but the number of decision variables in the optimization level *may be* greater than that in conventional NMPC. Actually, the conventional NMPC is a lowest-order (zero-order) parameterization; stepwise constants (manipulated variables), with no continuity in variables and their time derivatives. For example, the first-order (linear) parameterization of the vector of controls in the form of $\mathbf{u}(t_{i+1}-t_i)=\mathbf{A}+\mathbf{B}(t_{i+1}-t_i)$ (when $\mathbf{B}=\mathbf{0}$, conventional NMPC is recovered) requires the same number of decision variables ($b_i,...,b_{i+m-1}$: i=k,...,k+R) as in NMPC due to piecewise-continuity constraints on variables at points t_i ($a_i=u_{i-1}$). Similarly, the second-order (quadratic) parameterization of the vector of controls in the form of $\mathbf{u}(t_{i+1}-t_i)=\mathbf{A}+\mathbf{B}(t_{i+1}-t_i)+\mathbf{C}(t_{i+1}-t_i)^2$ requires again the same number of decision variables ($c_i,...,c_{i+m-1}$: i=k,...,k+R) as in NMPC due to piecewise-continuity constraints on variables and on their time derivatives at points t_i ($a_i=u_{i-1}$, and $du_i/dt=du_{i-1}/dt$). For higher order parameterizations (e.g., cubic), if the continuity conditions on consecutively higher-order time derivatives ($du^n_i/dt^n=du^n_{i-1}/dt^n$; n≥2) are not imposed, the number of decision variables optimized in NMPC/SPCCVLP gets larger compared to conventional NMPC. The formulation of the NMPC/SPCCVLP is given by Eqs.(25-38). The path constraints (Eq.31) are converted into a terminal equality constraint (Eq.35) by augmenting the set of ODEs with the single ODE given by Eq.34. Eqs.(36-38) indicate the piecewise continuity of the controls at the spline points over the prediction horizon.

$$\underset{\mathbf{u}(i),\ldots,\mathbf{u}(i+m-1)}{\textit{minimize}} \quad \Phi\left(\mathbf{u}(i)\right)=\int_{t_i}^{t_{k+R}}\left\|\mathbf{T}_k^{t,opt}(\infty)-\mathbf{T}_{MP}^{t}(i)\right\|dt \qquad i=k,\ldots,k+R \qquad (13)$$

$$\mathbf{T}_{MP}^{t}(i)=\mathbf{T}_{M}^{t}(i)+\mathbf{d}(k) \qquad i=k,\ldots,k+R \qquad (14)$$

$$\mathbf{d}(k)=\mathbf{T}_{P}^{t}(k)-\mathbf{T}_{M}^{t}(k) \qquad (15)$$

$$\dot{\mathbf{x}}(t,z)=\boldsymbol{f}\left(\mathbf{x}(t,z),\partial\mathbf{x}(t,z)/\partial z,\mathbf{u}(t),\mathbf{p},\mathbf{d}\right) \qquad t\in[k,\ldots,k+R] \qquad (16)$$

$$\mathbf{x}(k,z)=\bar{\mathbf{x}}(z) \qquad (17)$$

$$\Delta\mathbf{T}_{min}^{t,*}\le\left\{\mathbf{T}^{t}(t)-\bar{\mathbf{T}}^{t}\right\}\le\Delta\mathbf{T}_{max}^{t,*} \qquad t\in[k,\ldots,k+R] \qquad (18)$$

$$(1-r)\bar{\mathbf{u}}\le\mathbf{u}(i)\le(1+r)\bar{\mathbf{u}} \qquad i=k,\ldots,k+R \qquad (19)$$

$$-r^{*}\mathbf{u}(i)\le\Delta\mathbf{u}(i+1)\le r^{*}\mathbf{u}(i) \qquad i=k+1,\ldots,k+R \qquad (20)$$

$$\Delta\mathbf{u}(i+1)=\mathbf{u}(i+1)-\mathbf{u}(i) \qquad (21)$$

$$\mathbf{u}(i)=\mathbf{u}(k+m-1) \qquad \forall\, i>k+m-1 \qquad (22)$$

$$\dot{x}(t)=\left\|min\left\{0,\left(\mathbf{T}^{t}(t)-\bar{\mathbf{T}}^{t}+\Delta\mathbf{T}_{min}^{t,*}\right)\right\}\right\|+\left\|min\left\{0,\left(\bar{\mathbf{T}}^{t}-\mathbf{T}^{t}(t)+\Delta\mathbf{T}_{max}^{t,*}\right)\right\}\right\| \qquad t\in[k,\ldots,k+R] \qquad (23)$$

$$x(t)\big|_{k+R}=0 \qquad t=k+R \qquad (24)$$

B — Global Parameterization (SPCCVGP):

Compared to conventional NMPC, both the response of the plant can be made smoother and the number of decision variables in the optimization level can be decreased significantly if the manipulated variables are parameterized as continuous but global functions over the prediction horizon and treated as piecewise-continuous at points t_k and applied in a sliding mode to the plant at t_k. This approach should perform better than "manipulated-variable blocking" which is used to decrease computational load in conventional NMPC at the expense of performance deterioration. Higher order global parameterizations may perform better, but the number of decision variables (coefficients of global polynomials) in the optimization level gets greater than that in conventional NMPC, if the order of global polynomial is greater than $N_m\times m$ which is the number of decision variables in conventional NMPC (assuming that the same global polynomial form is used for all the manipulated variables). For example, the first-order (linear) global parameterization of the vector of controls in the form of $\mathbf{u}(t_i-t_k)=\mathbf{a}+\mathbf{b}(t_i-t_k)$ (i=k,...,k+R) requires only N_m decision variables over the prediction horizon t∈[k,...,k+R] due to piecewise-continuity constraints on variables at points t_k ($a_k=u_{k-1}$). Similarly, the second-order (quadratic) parameterization of the vector of controls in the form of $\mathbf{u}(t_i-t_k)=\mathbf{a}+\mathbf{b}(t_i-t_k)+\mathbf{c}(t_i-t_k)^2$ requires again only N_m decision variables due to piecewise-continuity constraints on variables and on their time derivatives at points t_k ($a_k=u_{k-1}$, and $du_k/dt=du_{k-1}/dt$). The formulation of the NMPC/SPCCVGP is given by Eqs.(25-35, 39-41).

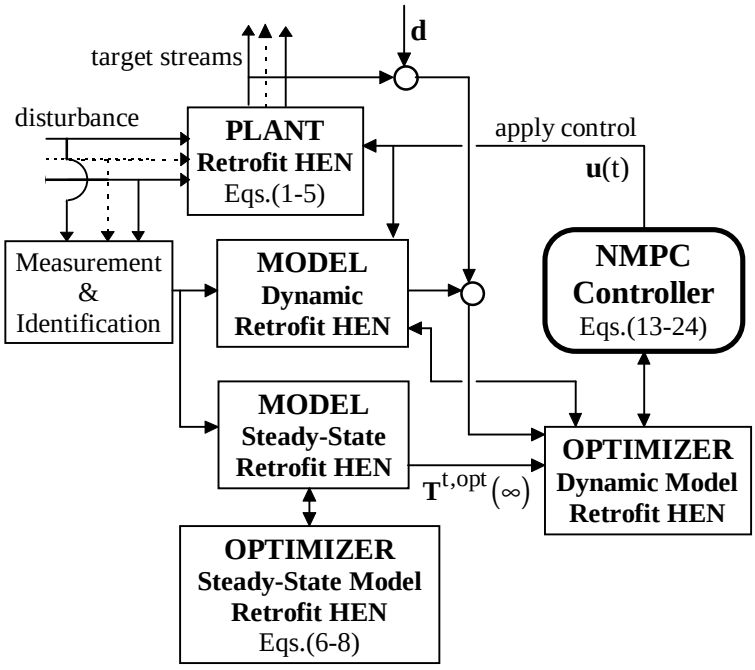


Figure 5. The NMPC scheme for control of retrofit HENs.

Example Control Problem with Plant/Model Mismatch

As an example, the control problem was defined as follows. When the consecutive source-temperature disturbances depicted in Fig.6 (0≤t<30: no disturbance, 30≤t<270: +5K in Hot-1, –5K in Cold-1 and –5K in Cold-2, 270≤t<510: no disturbance, 510≤t<750: +2K in Cold-1, 750≤t<1000: no disturbance) enter the HEN, keep the target temperatures of streams Hot-1 and Cold-1 at their nominal values given in Table 1 (hard targets), keep the target temperature of stream Hot-2 within ±5.5K and Cold-2 within ±4K, and keep the bypass openings within ±25% (r = 0.25) of their nominal values indicated in Fig.3. The SSOC problem, Eqs.(6-8), guarantees that the hard- and soft-target constraints are feasible for the retrofit

HEN at the post-disturbance steady-state. The source of the plant/model mismatch was considered as a significant +2% underestimation of the convective heat-transfer coefficients in the PDE models, Eqs.(9-10), of all the exchangers with respect to the plant. Table 2 lists some of the parameters used in the NMPC schemes.

Table 2. Some parameters used in NMPC schemes.

$\Delta t = t_{k+1} - t_k = 30$ s	m = 3 steps	R = 4 steps
$t_R - t_m = \Delta t$	r = 0.25	r* = 0.1

Fig.7 gives a comparison of NMPC with NMPC/SPCCVGP (global and *linear* parameterization), for the parameters in Table 2, in terms of CPU time (minutes), number of constraints (NMPC: 13 inequality and 1 equality; SPCCVGP: no inequality, 2 equality constraints), and number of optimization variables (NMPC: 12; SPCCVGP: 4 decision variables).

Fig.8 shows the response of the retrofit HEN and the controls implemented with the conventional NMPC scheme, with plant/model mismatch. The control scheme is capable of satisfying all the control objectives (steady-state and temporal hard/soft targets). However, the response is not smooth. The jumps in the target temperatures are due to stepwise implementation of the controls and the way the bypass-mixing points were modeled. These jumps cannot be avoided completely by imposing smaller velocity constraints on bypass openings.

Fig.9 shows the response of the retrofit HEN and the controls implemented with the NMPC/SPCCVGP scheme (global and *linear* parameterization), with plant/model mismatch. This control scheme as well is capable of satisfying all the control objectives (steady-state and temporal hard/soft targets). The response is quite smooth compared to conventional NMPC, and the jumps in the target temperatures are now completely eliminated.

Conclusions

Retrofit design of a HEN was performed considering placement of manipulated variables (bypasses) in order to increase HEN`s flexibility and resiliency. NMPC of the retrofit HEN modeled with PDEs was studied. A steady-state optimization algorithm, which determines feasible (optimal) post-disturbance target temperatures, was combined with the NMPC algorithm. The conventional NMPC scheme satisfied all the temporal and steady-state hard/soft target-temperature constraints even in the presence of a significant plant/model mismatch, however with nonsmooth response. A version of the classical NMPC scheme, NMPC/SPCCVGP, which has a piecewise-continuous *linear-global* parameterization of the control-vector, showed a superior performance with regard to smoothness of the response and significant reduction in computational load. *Quadratic-global* parameterization performed slightly better than the *linear-global* parameterization in terms of the smoothness of the response at no additional computational load. *Local* parameterizations (linear or quadratic) also gave smoother responses, however with no benefit with respect to computational load compared to the load in the conventional NMPC.

$$\underset{\mathbf{u}(i),\ldots,\mathbf{u}(i+m-1)}{minimize}\ \Phi\left(\mathbf{u}(i)\right) = \int_{t_i}^{t_{k+R}} \left\| \mathbf{T}_k^{t,opt}(\infty) - \mathbf{T}_{MP}^{t}(i) \right\| dt \quad i=k,\ldots,k+R \qquad (25)$$

$$\mathbf{T}_{MP}^{t}(i) = \mathbf{T}_{M}^{t}(i) + \mathbf{d}(k) \quad i=k,\ldots,k+R \qquad (26)$$

$$\mathbf{d}(k) = \mathbf{T}_{P}^{t}(k) - \mathbf{T}_{M}^{t}(k) \qquad (27)$$

$$\dot{\mathbf{x}}(t,z) = \boldsymbol{f}\left(\mathbf{x}(t,z), \partial\mathbf{x}(t,z)/\partial z, \mathbf{u}(t), \mathbf{p}, \mathbf{d}\right) \quad t \in [k,\ldots,k+R] \qquad (28)$$

$$\mathbf{x}(k,z) = \bar{\mathbf{x}}(z) \qquad (29)$$

$$\Delta\mathbf{T}_{min}^{t,*} \le \left\{ \mathbf{T}^{t}(t) - \bar{\mathbf{T}}^{t} \right\} \le \Delta\mathbf{T}_{max}^{t,*} \quad t \in [k,\ldots,k+R] \qquad (30)$$

$$(1-r)\bar{\mathbf{u}} \le \mathbf{u}(t) \le (1+r)\bar{\mathbf{u}} \quad t \in [k,\ldots,k+R] \qquad (31)$$

$$\dot{x}(t) = \left\| min\left\{0, \left(\mathbf{T}^{t}(t) - \bar{\mathbf{T}}^{t} + \Delta\mathbf{T}_{min}^{t,*} \right)\right\}\right\| + \left\| min\left\{0, \left(\bar{\mathbf{T}}^{t} - \mathbf{T}^{t}(t) + \Delta\mathbf{T}_{max}^{t,*} \right)\right\}\right\| \quad t \in [k,\ldots,k+R] \qquad (32)$$

$$x(t)\big|_{k+R} = 0 \quad t=k+R \qquad (33)$$

$$\dot{y}(t) = \left\| max\left\{0, \left(\left| \mathbf{u}(t) - \bar{\mathbf{u}} \right| - r\bar{\mathbf{u}} \right)\right\}\right\| \quad t \in [k,\ldots,k+R] \qquad (34)$$

$$y(t)\big|_{k+R} = 0 \quad t=k+R \qquad (35)$$

for SPCCVLP:

$$\mathbf{u}(t) = \boldsymbol{P}_i(t) \quad t \in [t_i,\ldots,t_{i+1}] \qquad (36)$$

$$\boldsymbol{P}_i(t) = \boldsymbol{P}_{i-1}\left(t^-\right) \quad t^- \in [t_{i-1},\ldots,t_i] \qquad (37)$$

$$d\boldsymbol{P}_i(t)/dt = d\boldsymbol{P}_{i-1}\left(t^-\right)/dt \quad t^- \in [t_{i-1},\ldots,t_i] \qquad (38)$$

for SPCCVGP:

$$\mathbf{u}(t) = \boldsymbol{P}_k(t) \quad t \in [t_k,\ldots,t_{k+R}] \qquad (39)$$

$$\boldsymbol{P}_k(t) = \boldsymbol{P}_{k-1}\left(t^-\right) \quad t^- \in [t_{k-1},\ldots,t_{k-1+R}] \qquad (40)$$

$$d\boldsymbol{P}_k(t)/dt = d\boldsymbol{P}_{k-1}\left(t^-\right)/dt \quad t^- \in [t_{k-1},\ldots,t_{k-1+R}] \qquad (41)$$

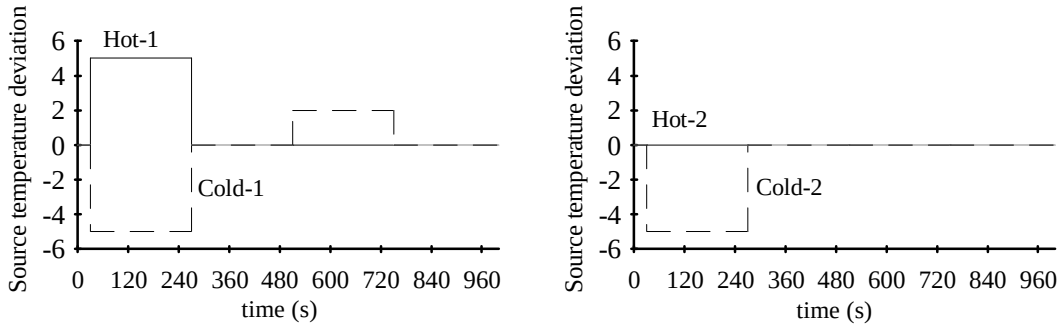


Figure 6. Consecutive disturbances introduced in the source-stream temperatures of the HEN.

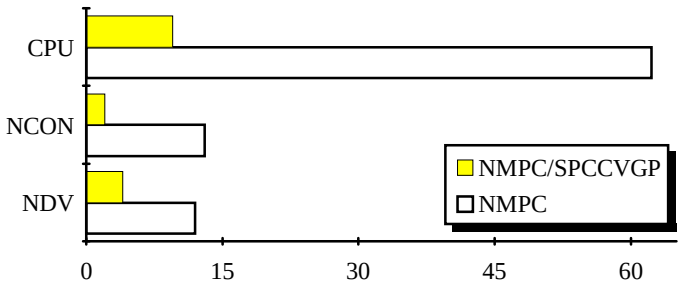


Figure 7. Comparison of NMPC with NMPC/SPCCVGP in terms of CPU time, number of constraints, and number of optimization variables.

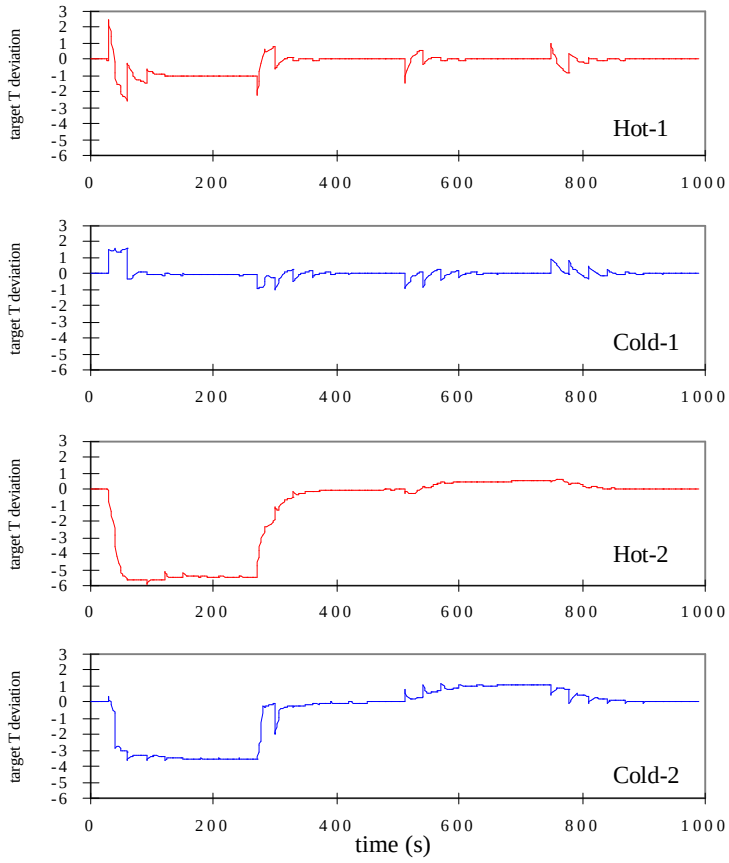


Figure 8.a. Target temperature deviations from nominal values under conventional NMPC scheme, with plant/model mismatch.

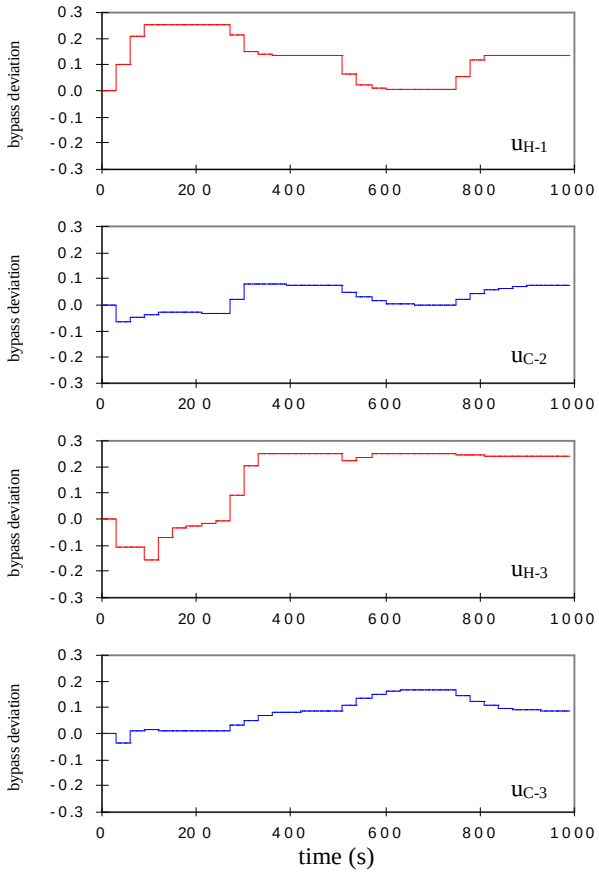


Figure 8.b. Deviations in bypass fractions relative to nominal values under conventional NMPC scheme, with plant/model mismatch.

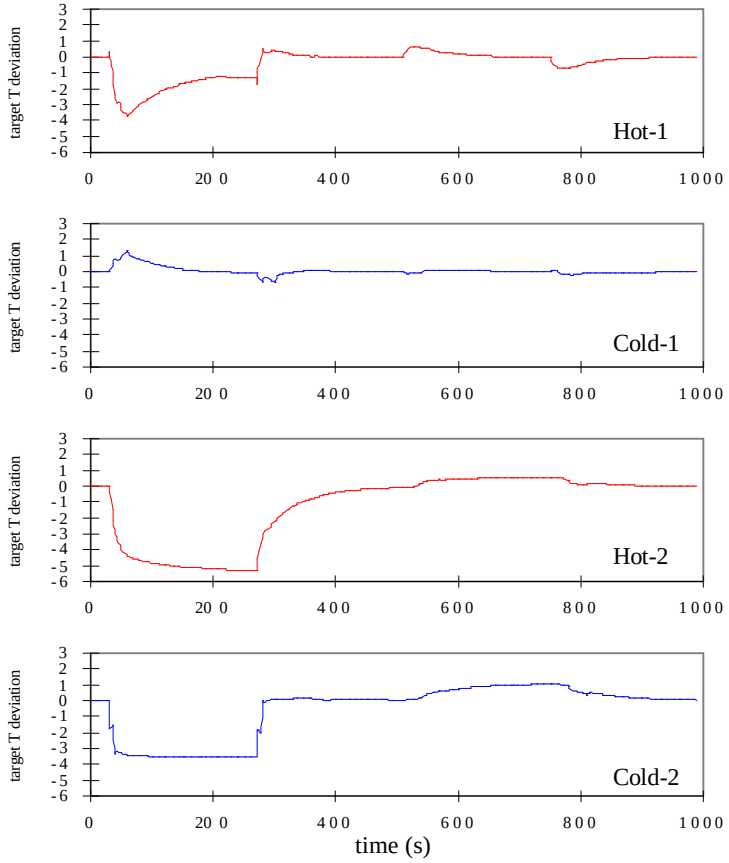


Figure 9.a. Target temperature deviations from nominal values under NMPC/SPCCVGP scheme (global and *linear* parameterization), with plant/model mismatch.

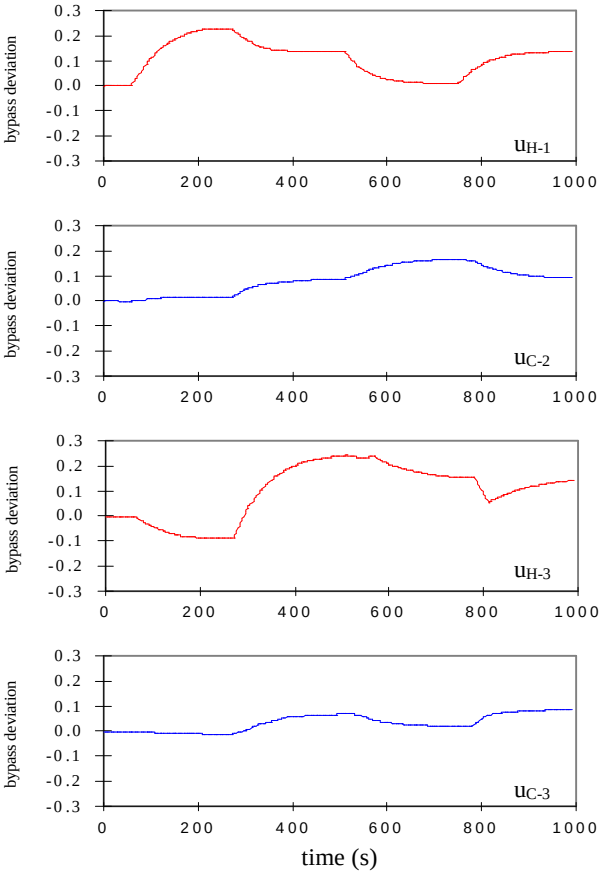


Figure 9.b. Deviations in bypass fractions relative to nominal values under NMPC/SPCCVGP scheme (global and *linear* parameterization), with plant/model mismatch.

Notation

a	surface area of tube per unit length
A	heat-exchanger area or cross-sectional area
C_p	heat capacity
d	disturbance vector accounting for plant/model mismatch
h	individual heat transfer coefficient
k	current time step
K_c	proportionality constant in PI controller
m	number of manipulated variable moves in the future
N_d	number of disturbance directions
N_{HEX}	number of heat exchangers in the network
N_m	number of manipulated variables
N_t	number of targets
N_T	number of tubes
p	vector of model parameters
r	fraction for bypass-opening bounds (for steady-state constraints)
r*	fraction for bypass-opening bounds (for temporal constraints)
R	prediction horizon
S	flexibility index (deviations from nominal source-stream temperatures)
t	time
T	temperature
ΔT^a	minimum-approach temperature
$\Delta T^{t,*}$	temporal constraints on target temperatures
u	bypass fraction
u	vector of bypass fractions
U	overall heat-transfer coefficient
v	velocity
x	state variables
z	axial position
∞	steady-state value
ρ	density

Subscript

C	cold (shell) side
H	hot (tube) side
m	m^{th} bypass stream
M	model
MP	model prediction
n	n^{th} heat exchanger
P	plant

Superscript

j, k	disturbance direction identifier
0	zero-disturbance value
opt	optimum
s	source
t	target
‾	nominal value (zero-disturbance value)

References

1. Boyacý, C., D. Uztürk, A.E.Þ. Konukman, U. Akman, “Dynamics and Optimal Control of Flexible Heat-Exchanger Networks”, *Computers Chem. Engng.*, Suppl. B, Vol.20, S775-S780 (1996)
2. Uztürk, D., A.E.Þ. Konukman, C. Boyacý, U. Akman, “Operability of an Autothermal Reactor Linked to a Flexible Heat-Exchanger Network”, *Computers Chem. Engng.*, Suppl. B, Vol.20, S943-S948 (1996)
3. Konukman, A.E.Þ., U. Akman, M.C. Çamurdan, “Optimal Design of Controllable Heat-Exchanger Networks Under Multi-Directional Resiliency-Target Constraints”, *Computers Chem. Engng.*, Suppl., Vol.19, S149-S154 (1995)
4. Uztürk D., U. Akman, “Centralized and Decentralized Control of Retrofýt Heat-Exchanger Networks”, *Computers Chem. Engng.*, Suppl., Vol.21, S373-S378 (1997)
5. Uztürk, D., “Frequency-Domain Analysis and Control of Retrofit Heat-Exchanger Networks”, M.Sc. thesis, Boðaziçi University (1996)
6. Yee, T.F., and Grossmann, I.E., “Simultaneous optimization models for heat integration - II: Heat exchanger network synthesis.”, *Computers Chem. Engng.*, Vol.10, pp.1165-1183 (1990)
7. Boyacý, C., “Dynamics and Optimal Control of Flexible Heat-Exchanger Networks”, M.Sc. thesis, Boðaziçi University (1995)
8. Raman, R., *Chemical Process Computations*, Elsevier, New York (1985)
9. Bequette, B.W., “Nonlinear Control of Chemical Processes: A Review”, *I&EC Res.*, Vol.30, No.7, pp.1391-1413 (1991)
10. Garcia, C.E., Prett, D.M., Morari, M., “Model Predictive Control: Theory and Practice - a Survey”, *Automatica*, Vol.25, No.3, pp.335-348 (1989)
11. Oliveira, N.M.C., Biegler, L.T., “An Extension of Newton-type Algorithms for Nonlinear Process Control”, *Automatica*, Vol.31, No.2, pp.281-286 (1995)
12. Li, W.C., Biegler, L.T., “Process Control Strategies for Constrained Nonlinear Systems”, *I&EC Res.*, Vol.27, No.8, pp.1421-1433 (1988)

Acknowledgment

Financial supports provided by TÜBÝTAK (The Scientific and Technical Research Council of Turkey) (Project No: MÝSAG-83) and the Boðaziçi University Research Fund (Project No: 94A0525) are gratefully acknowledged.